

doi.org/10.3114/fuse.2021.08.13

## On six African species of *Lyomyces* and *Xylodon*

I. Viner<sup>1\*</sup>, F. Bortnikov<sup>2</sup>, L. Ryvardeen<sup>3</sup>, O. Miettinen<sup>1</sup>

<sup>1</sup>Botanical Museum, Finnish Museum of Natural History, University of Helsinki, P.O. Box 7, 00014, Finland

<sup>2</sup>Faculty of Biology, Lomonosov Moscow State University, Leninskie Gory 1/12, 119234 Moscow, Russia

<sup>3</sup>Institute of Biological Sciences, University of Oslo, P.O. Box 1066, Blindern, N.0316 Oslo, Finland

\*Corresponding author: ilya.viner@helsinki.fi

### Key words:

Corticoidiis  
new species  
phylogeny  
taxonomy

**Abstract:** We studied a number of sub-Saharan collections of corticioid *Xylodon* and *Lyomyces* species, including several types. Morphological descriptions and molecular analyses based on the ribosomal DNA loci nuc rDNA ITS1-5.8S-ITS2 and when possible nuc 28S rDNA, allow us to introduce four new species: *L. densiusculus*, *X. angustisporus*, *X. dissiliens*, and *X. laxiusculus*. DNA barcodes for *X. submucronatus* and *X. pruniaceus* are published for the first time and *X. pruniaceus* is re-described.

**Citation:** Viner I, Bortnikov F, Ryvardeen L, Miettinen O (2021). On six African species of *Lyomyces* and *Xylodon*. *Fungal Systematics and Evolution* 8: 163–178. doi: 10.3114/fuse.2021.08.13

**Received:** 1 October 2021; **Accepted:** 8 November 2021; **Effectively published online:** 24 November 2021

**Corresponding editor:** P.W. Crous

## INTRODUCTION

Sub-Saharan Africa remains poorly explored for fungi due to the lack of taxonomists and scientific infrastructure. Yet, the region is a hotspot for discovering new species (Cheek *et al.* 2020). In this situation, local and global extinction events caused by habitat loss or climate change may occur unnoticed simply because science has not recorded the existence of species (Cheek *et al.* 2018). Consequently, nature conservation strategies cannot consider fungal diversity. Other than fungal inventories based on the morphological identification of sporocarps, an ample source of species records to work with is DNA sequences from environmental samples. Those have an advantage of spotting fungi in stages other than morphologically identifiable sporocarps. Inconveniently, such DNA fragments often cannot be precisely attributed to species names. They may represent already described taxa without DNA barcodes or truly undescribed species known only from environmental sequences. Environmental sequences cannot be given taxonomic names because of the lack of a physical voucher specimen deposited in a fungarium (Lücking & Hawksworth 2018). For these reasons, we find it important to work towards filling the gaps in our knowledge of African mycota.

*Lyomyces* and *Xylodon* are two closely related genera with unclear molecular and morphological borders. These genera had been treated in *Hyphodontia* for a couple of decades until Hjortstam & Ryvardeen (2007, 2009) re-introduced them. Together they are the most species-rich and abundant group in the family *Schizoporaceae* (*Hymenochaetales*, *Basidiomycota*) worldwide. Despite their great abundance, we are aware of only six currently recognised species described from Africa including Réunion. We describe here four new species in this group and provide molecular data for two already existing taxa, which previously lacked DNA barcodes.

## MATERIALS AND METHODS

### Morphological methods

Type material and specimens from fungaria H, O, and GB were studied. Fungarium abbreviations are given according to Index Herbariorum (Thiers). Microscopic methods were described in Miettinen *et al.* (2006). All measurements were made in Cotton Blue (CB, Merck 1275; Kenilworth, New Jersey) with phase contrast illumination (1 250 ×), which allowed reporting them with 0.1 μm precision. The benefits of phase contrast illumination over bright-field microscopy are explained by Stein (1969). The following abbreviations were used in microscopic descriptions: L – mean spore length; W – mean spore width; Q – mean L/W ratio; n – number of elements (basidiospores, basidia, cystidia, and hyphae) measured, which are followed by the number of specimens studied. We excluded 5 % of measurements from each end of the range representing variation of basidiospores and cystidia. Excluded extreme values were indicated in parentheses when they strongly differed from the lower or higher 95 % percentile.

### DNA extraction and sequencing

Total genomic DNA was extracted from herbarium specimens using a CTAB-chloroform extraction protocol (Kutuzova *et al.* 2017). We used standard as well as self-designed primers (Table 1) to amplify complete nuc rDNA ITS1-5.8S-ITS2 (ITS) and in some cases nuc 28S rDNA (28S) for all focal taxa. After amplification PCR products were run on a 1.5 % agarose gel stained with Gel Red staining (Biotium, Fremont, California) and visualized under UV light. PCR products were purified from agarose gels using a Fermentas Genomic DNA Purification Kit (Thermo Fisher

**Table 1.** Primers used in this study.

Primer name	Sequence	Target DNA locus	Binding site	Direction	Reference
ITS5	GGAAGTAAAAGTCGTAACAAGG	ITS, ITS1	18S	fwd	White <i>et al.</i> (1990)
ITS2	GCTGCGTTCTTCATCGATGC	ITS1	5.8S	fwd	White <i>et al.</i> (1990)
58A1F	GCATCGATGAAGAACGC	ITS2	5.8S	fwd	Martin & Rygiewicz (2005)
ITS2.2rXyl	TTATCACACCGCATATATGC	ITS2	ITS2	rev	this study
ITS2.2fXyl	CTTCYCTTGAATGYATTA	ITS2	ITS2	fwd	this study
ALR0.2	GATATGCTTAAGTTCAGCGGG	ITS, ITS2	28S	rev	Riebesehl & Langer (2017)
LR22	CCTCACGGTACTTGTTGCT	ITS	28S	rev	Vilgalys lab, Duke University ( <a href="https://sites.duke.edu/vilgalyslab/files/2017/08/rDNA-primers-for-fungi.pdf">https://sites.duke.edu/vilgalyslab/files/2017/08/rDNA-primers-for-fungi.pdf</a> )
JS1	CGCTGAACTTAAGCATAT	28S	28S	fwd	Landvik (1996)
LR7	TACTACCACCAAGATCT	28S	28S	rev	Hopple & Vilgalys (1994)

Scientific, Waltham, Massachusetts). Sequencing reactions were performed on an ABI 3730XL DNA analyzer (Applied Biosystems) by MacroGen (Amsterdam, the Netherlands).

A number of additional 28S sequences used in the analyses came from partial genomes. The corresponding DNA extractions were sequenced with the aid of NextSeq 550 sequencing using the Nextera kit at Biomedicum Functional Genomics Unit (Helsinki, Finland). The assessment of read quality and their cleaning was performed using the FastQC and FastP tools (Chen *et al.* 2018). For the identification of 28S from the fungal genomes, the cleaned reads were mapped to nrDNA and 28S sequences and then were assembled using the SPADES (Bankevich *et al.* 2012) and MEGAHIT assemblers (Li *et al.* 2015). Additionally, to check the homology of the predicted genes, nrDNA and 28S were aligned to the assembled genomes using LASTz (Harris 2007). Sequences with the identity of at least 50 % and the coverage of 70 % were extracted. All newly produced sequences used in this study have been deposited in GenBank (Table 2).

### Phylogenetic analyses

Extremely high diversity of ITS sequences in the focal genera precluded attempts to construct a reliable all-encompassing alignment for this locus, even if *Lyomyces* and *Xylodon* are analysed separately. Phylogenies produced based on such alignments became highly sensitive to the taxon sampling and the selected alignment algorithm. Therefore, we produced a reliably aligned dataset based on more conservative locus 28S (D1–D4) to show the phylogenetic placement of focal taxa with available nuclear LSU sequences. Then we constructed three additional ITS alignments for *L. densiusculus*, *X. laxiusculus*, and *X. submucronatus*, which belonged to lineages abundant in GenBank (Benson *et al.* 2018) as of 1 July 2021. Only sequences that could be reliably aligned were used in the ITS analyses. This corresponded to 89–93 % threshold of pairwise similarity to our newly produced sequences. As ITS of *X. angustisporus*, *X. dessiliens*, and *X. pruniaceus* had no close matches in public databases, these sequences were not used for building the ITS-based phylogenies.

Alignments were calculated through the MAFFT v. 7.429 online server (<https://mafft.cbrc.jp/alignment/server/>) using the L-INS-I strategy (Katoh *et al.* 2017). After removing unalignable fragments, the length of the alignment and the number of parsimony informative characters were correspondingly 1 280

and 235 bp for the 28S alignment; 570 and 54 bp for the *L. densiusculus* alignment; 660 and 51 bp for the *X. laxiusculus* alignment; 550 and 85 bp for the *X. submucronatus* alignment. The full alignments with annotation of the excluded characters were deposited at TreeBASE (study 28841).

We inferred rooted phylogenetic trees with maximum likelihood (ML) and Bayesian Inference (BI). Nucleotide substitution models for BI were chosen with TOPALI v. 2.5 (Milne *et al.* 2008) based on the Bayesian information criterion (BIC). We performed BI using MrBayes v. 3.2 (Ronquist *et al.* 2012). In these analyses three parallel runs with four chains each and other default parameters were run for one million generations. A burn-in of 25 % was used in the final analyses, ensuring the average standard deviation of split frequencies had reached < 0.01 for all data sets. Support at nodes was indicated when posterior probabilities were  $\geq 0.8$ . For ML analyses, IQ-TREE v. 1.2.2 (Nguyen *et al.* 2015) with the best-fitted model option was used. Bootstrapping was performed using the standard nonparametric bootstrap algorithm with the number of replicates set to 1 000. Support at nodes was indicated with bootstrap values  $\geq 70$  %.

### RESULTS

Bayesian Inference and ML returned similar topologies and relevant support values from these analyses were indicated at nodes in Figs 1–4. The 28S analysis returned a tree with a clade consisting of *Xylodon* and *Lyomyces* distinct from *Hastodontia* and *Fasciodontia* (Fig. 1). All *Lyomyces* taxa were confined to one clade supported only by BI. Basal relationships within the *Xylodon/Lyomyces* cluster were not resolved. Newly described *X. angustisporus* occupied a place at the deepest split of the *Xylodon/Lyomyces* cluster.

Our ITS analyses showed that *X. submucronatus* occurred as a sister taxon to *X. rimosissimus* (Fig. 2), *L. densiusculus* ended up in the same clade with *L. fimbriatus* (Fig. 3), while *X. laxiusculus* formed a subclade with *X. subclavatus* (Fig. 4). As blasting ITS of newly described *X. angustisporus* and *X. dissiliens* returned no close hits that would have allowed building a reliable ITS alignment, we included these species only in the 28S analysis (Fig. 1). *X. pruniaceus* – sequenced for the first time in this study – turned out to be the single close relative of *X. angustisporus* in our dataset, with a 96.4 % ITS similarity, or only 22 bp difference.

**Table 2.** Sequences used in this study. Sequences marked with \* were produced for this study.

Species	Specimen	ITS	28S
<i>Fasciodontia bugellensis</i>	Larsson 8195	OK273855*	OK273855*
<i>Fasciodontia</i> sp.	Zhao 6280	–	MZ146327
<i>Hastodontia hastata</i>	Larsson 14646	MH638232	MH638232
<i>Lyomyces</i> aff. <i>orientalis</i>	Boidin 383	MH857295	–
<i>Lyomyces bambusinus</i>	Zhao 4831	–	MW264919
<i>Lyomyces crustosus</i>	Spirin 12603	OK273832*	OK273832*
<i>Lyomyces densiusculus</i>	Ryvarden 44818	OK273853*	OK273853*
<i>Lyomyces elaeidicola</i>	He 6360	–	MW507035
	He 6378	–	MW507036
<i>Lyomyces fimbriatus</i>	Wu 910620-7	MK575209	–
	Wu 911204-4	MK575210	–
<i>Lyomyces griseliniae</i>	Larsson 5289	OK273851*	OK273851*
<i>Lyomyces leptocystidiatus</i>	Zhao 20170815-30	MT319427	–
	Zhao 20170815-43	MT319428	–
	Zhao 20170814-14	MT319429	–
	Zhao 20170815-2	MT319430	–
	Zhao 20170818-1	MT319431	–
	Zhao 20170814-8	MT319432	–
	Zhao 20170818-8	MT319433	–
	Zhao 20170908-14	MT319434	–
<i>Lyomyces macrosporus</i>	Zhao 20170818-9	MT319435	–
	He 6179	–	MW507034
<i>Lyomyces microfasciculatus</i>	Zhao 4516	–	MW264920
	He 2651	–	MW507027
<i>Lyomyces orientalis</i>	Zhao 5109	–	MW264921
	He 3616	–	MW507030
<i>Lyomyces pruni</i>	He 3686	–	MW507031
	Spirin 12682	OK273833*	OK273833*
<i>Lyomyces sambuci</i>	Miettinen 11705	OK273852*	OK273852*
	He 6108	–	MW507033
	He 6576	–	MW507037
<i>Lyomyces</i> sp.	Zhao 8188	MW713744	–
	Zhao 17855	MW713745	–
	Burdsall HHB-19410	MW740296	–
	Burdsall HHB-19323	MW740297	–
	Zhao 10474	–	MZ262525
	Zhao 4299	–	MW713731
	Zhao 4352	–	MW713732
	Zhao 4385	–	MZ262521
	Zhao 4394	–	MW713733
	Zhao 4725	–	MZ262522
	Zhao 6224	–	MZ262523
	Zhao 6431	–	MZ262526
	Zhao 6442	–	MZ262527
	Zhao 6474	–	MZ262528
	Zhao 6483	–	MZ262529
	Zhao 6565	–	MZ262531
	Zhao 8188	–	MW713736

Table 2. (Continued).

Species	Specimen	ITS	28S
	Zhao 9784	–	MW713735
<i>Lyomyces vietnamensis</i>	He 3260	–	MW507028
<i>Lyomyces wuliangshanensis</i>	He 3498	–	MW507029
	He 4765	–	MW507032
<i>Xylodon</i> aff. <i>borealis</i>	UC2022850	KP814307	–
<i>Xylodon angustisporus</i>	Ryvarden 50691b	OK273831*	OK273831*
<i>Xylodon apacheriensis</i>	Miettinen 16686	OK273835*	OK273835*
<i>Xylodon asperus</i>	clone BF-OTU19	AM902054	–
	Nilsson 2004b	DQ873606	DQ873607
	Langer 3257	EU583424	–
	NFLI 2000-112/1	JQ358805	–
	UC2023164	KP814364	–
	UC2023169	KP814365	–
	UC2023187	KP814366	–
	Dai 14824	KY290980	–
	NIBIO 2016-0924/1	MF511090	–
	Zhao 1035	MG231619	–
	Zhao 1068	MG231620	–
	Zhao 1070	MG231621	–
	Zhao 1076	MG231622	–
	Zhao 1078	MG231623	–
	Zhao 1154	MG231624	–
	Zhao 1168	MG231625	–
	Zhao 1169	MG231626	–
	Zhao SWFU 006420	MK809500	–
	Zhao 6543	MW940726	–
	Spirin 11923	OK273838*	OK273838*
<i>Xylodon attenuatus</i>	Spirin 8775	MH324476	–
	Spirin 8714	OK273839*	OK273839*
<i>Xylodon bambusinus</i>	Zhao 11211	MW394658	MW394651
	Zhao 11219	MW394659	MW394653
	Zhao 11310	MW394660	MW394655
	Zhao 11215	MW394661	MW394652
	Zhao 11224	MW394662	MW394654
<i>Xylodon borealis</i>	Spirin 10911	OK273846*	OK273846*
<i>Xylodon crystalliger</i>	KUN3347	OK273842*	OK273842*
<i>Xylodon cystidiatus</i>	Savchenko AS171128/1625B	OK273850*	OK273850*
<i>Xylodon detriticus</i>	Miettinen 22106	OK273844*	OK273844*
<i>Xylodon dissiliens</i>	Ryvarden 44817	OK273856*	OK273856*
<i>Xylodon flaviporus</i>	MA Fungi 79440	MH260071	MH260066
<i>Xylodon hypodontinus</i>	Savchenko AS171124/1235	OK273848*	OK273848*
<i>Xylodon laurentianus</i>	DLL2009-049	JQ673187	–
	DLL2009-082	JQ673188	–
	DLL2009-087	JQ673189	–
	clone CMH177	KF800268	–
	DLL2011-142	KJ140643	–
	HHB_719	KY962845	–
	Zhao 140	MG231647	–

Table 2. (Continued).

Species	Specimen	ITS	28S
	Russell 8118	MK575271	–
<i>Xylodon laxiusculus</i>	Ryvarden 44877	OK273827*	–
<i>Xylodon nespori</i>	Nordon 030915	DQ873622	DQ873622
	Viner 2019_59	OK273834*	OK273834*
<i>Xylodon niemelaei</i>	Savchenko TU114922	OK273836*	OK273836*
	GC 1508-146	–	KX857816
<i>Xylodon nongravis</i>	Spirin 5615	OK273849*	OK273849*
<i>Xylodon nothofagi</i>	ICMP 13839	AF145582	MH260064
<i>Xylodon ovisporus</i>	ICMP 13835	AF145586	MH260063
	KUC8140	JGI	JGI
<i>Xylodon paradoxus</i>	Oivanen PO109	OK273843*	OK273843*
<i>Xylodon patagonicus</i>	strain P.CH-4	KF562013	–
	MA-Fungi 90705	KY962835	–
	MA-Fungi 90702	KY962836	–
	MA-Fungi 90707	KY962837	–
	MA-Fungi 90704	KY962840	–
	MA-Fungi 90703	KY962841	–
	Smith MES-2446	MH930325	–
<i>Xylodon pruinus</i>	Viner 2019_21	OK273845*	OK273845*
	Nilsson 990902	DQ677507	DQ677507
<i>Xylodon pruniaceus</i>	Ryvarden 11251	OK273828*	–
<i>Xylodon pseudolanatus</i>	HHB-10703-Sp	OK273847*	OK273847*
<i>Xylodon pseudotropicus</i>	Otto Miettinen 16558.2	OK273854*	OK273854*
<i>Xylodon quercinus</i>	Miettinen 15050.1	KT361632	–
	Larsson 11076	KT361633	–
	Boidin 4014	MH858169	–
	MA-Fungi 91815	MT158722	–
	MA-Fungi 91816	MT158723	–
	clone 4248_520	MT236714	–
	Spirin 12030	OK273841*	OK273841*
<i>Xylodon raduloides</i>	Dai 12631	KT203307	–
	MA-Fungi 12864	KY962820	–
	MA-Fungi 12877	KY962821	–
	MA-Fungi 22499	KY962822	–
	MA-Fungi 22513	KY962823	–
	MA-Fungi 75310	KY962825	–
	MA-Fungi 70457	KY962827	–
	MA-Fungi 78658	KY962828	–
	MA-Fungi 75272	KY962829	–
	MA-Fungi 79314	KY962830	–
	MA-Fungi 35643	KY962831	–
	MA-Fungi 12778	KY962832	–
	MA-Fungi 75244	KY962833	–
	MA-Fungi 608	KY962838	–
	NY s.n.	KY962843	–
	MA-Fungi 90709	KY962844	–
	Riebesehl KAS-JR03	MH880222	–
	Riebesehl KAS-JR09	MH880223	–

Table 2. (Continued).

Species	Specimen	ITS	28S
	Riebesehl KAS-JR26	MH880225	–
	clone 4248_300	MT236523	–
	Polemis EP.18-A1543	MT458537	–
	Dai 12631	–	KT203328
<i>Xylodon ramicida</i>	Spirin 7664	NR138013	–
<i>Xylodon rimosissimus</i>	Ryberg 021031	DQ873627	–
	pIB4D	HM136630	–
	clone 201	KC785580	–
	Lindner 2011-081	KJ140600	–
	UC2023147	KP814193	–
	UC2023148	KP814194	–
	UC2022842	KP814311	–
	UC2023109	KP814414	–
	Zhao 1487	MG231649	–
	Russell 8120	MK575252	–
	Dirks PUL F24614	MW448610	–
	Miettinen 12026.1	OK273840*	OK273840*
<i>Xylodon</i> sp.	Langer 3365	DQ340324	–
	Larsson 12386	DQ873612	DQ873612
	Berglund 1117	DQ873633	DQ873634
	clone F126	JX981881	–
	Larsson 6686	LN714553	–
	Zhao SWFU 006465	MK809410	–
	LWZ 20180904-28	MT319674	–
	Zhao 16090	MW566132	–
	Zhao 18342	–	MW980779
	Zhao 18379	–	MW980780
	Zhao 18394	–	MW980781
	Zhao 210	–	MN654918
	Zhao 214	–	MN654919
	Zhao 215	–	MN654920
<i>Xylodon spathulatus</i>	Spirin 12007	OK273837*	OK273837*
	Wu 1307-42	–	KX857810
<i>Xylodon subclavatus</i>	TUB-FO 42167	MH880232	–
<i>Xylodon submucronatus</i>	Ryvarden 9322b	OK273829*	–
	Renvall 1602	OK273830*	–
<i>Xylodon subtropicus</i>	Wu 1508-2	KX857806	–
	Zhao 20180512-15	MT319539	–
<i>Xylodon verecundus</i>	Larsson 12261	–	DQ873643
<i>Xylodon xinpingensis</i>	Zhao 9125	–	MW394649
	Zhao 9174	–	MW394650
<i>Xylodon yarraensis</i>	LWZ 20180510-4	MT319635	–
	LWZ 20180510-16	MT319637	–
	LWZ 20180510-19	MT319638	–
	LWZ 20180510-5	MT319639	–
	LWZ 20180509-7	MT319640	–
	LWZ 20180512-21	MT319641	–
	LWZ 20180512-22	MT319642	–

Table 2. (Continued).

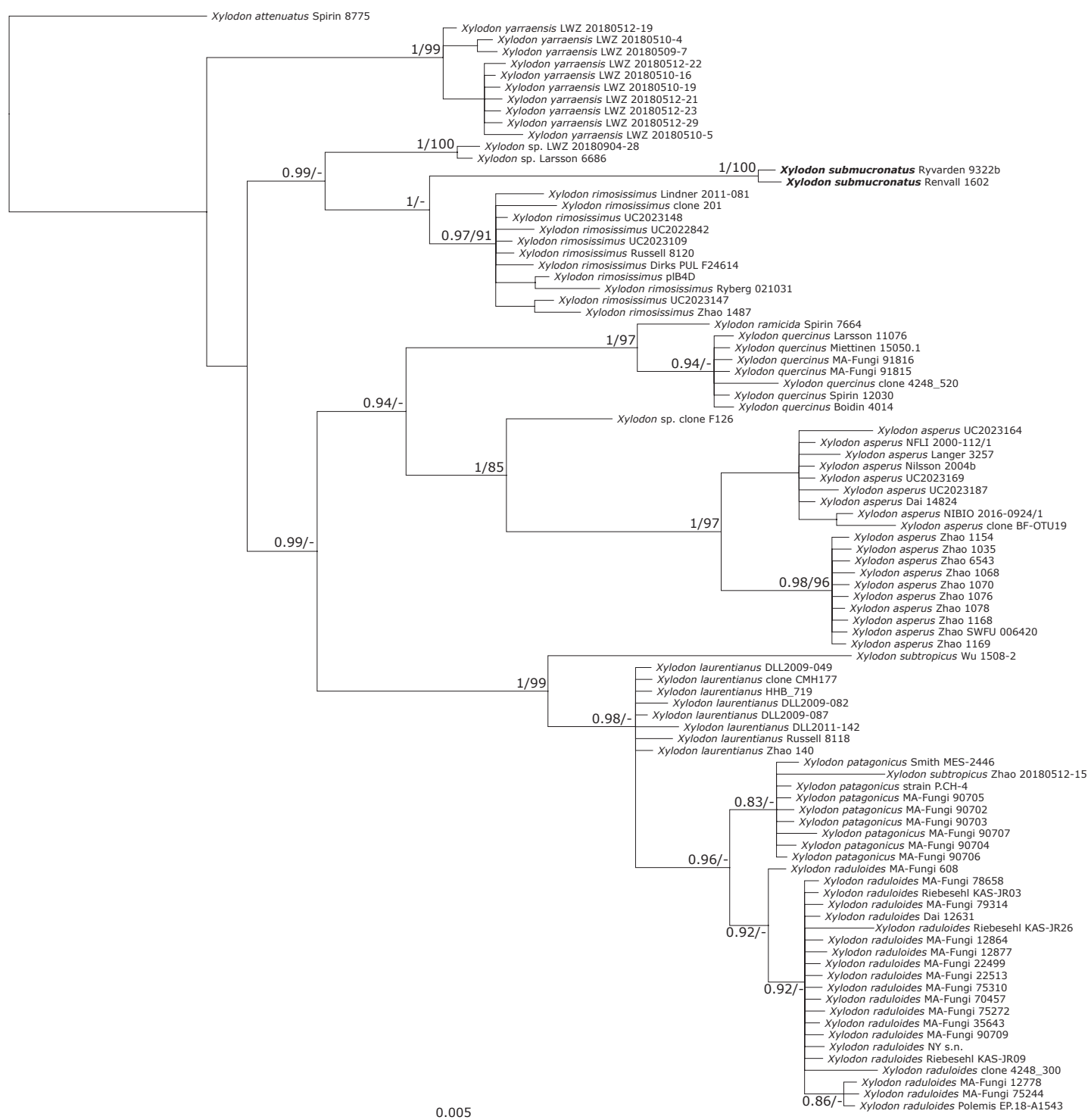
Species	Specimen	ITS	28S
	LWZ 20180512-23	MT319643	–
	LWZ 20180512-29	MT319644	–
	LWZ 20180512-19	MT319645	–



Fig. 1. Phylogenetic relationships of *Xylodon* and *Lyomyces* inferred from 28S sequences using BI analysis. Bayesian posterior probabilities followed by ML bootstrap values are shown at nodes; branch lengths reflect estimated number of changes per site.

There were three 28S sequences with questionable species assignment. Zhao 210 (GenBank MN654918), Zhao 214 (GenBank MN654919), and Zhao 215 (GenBank MN654920) belong to one of the *Xylodon* clades despite being published as *Trechispora yunnanensis* (*Trechisporales*, *Basidiomycota*). The *X. submucronatus* tree also contained two similarly problematic ITS sequences. MA-Fungi 91816 (GenBank MT158723) and MA-Fungi 91815 (GenBank MT158722) clearly belong to *X. quercinus* despite being published as *X. magallanesii*.

Morphological differences between species in *Xylodon* and *Lyomyces* complex are often small, but we have found reliable characters to separate all newly described species from other African material we are aware of. We introduce four new species supported by the results of our molecular and morphological analyses.



**Fig. 2.** Phylogenetic relationships of *Xylodon submucronatus* and allied taxa inferred from ITS sequences using BI analysis. Bayesian posterior probabilities followed by ML bootstrap values are shown at nodes; branch lengths reflect estimated number of changes per site.



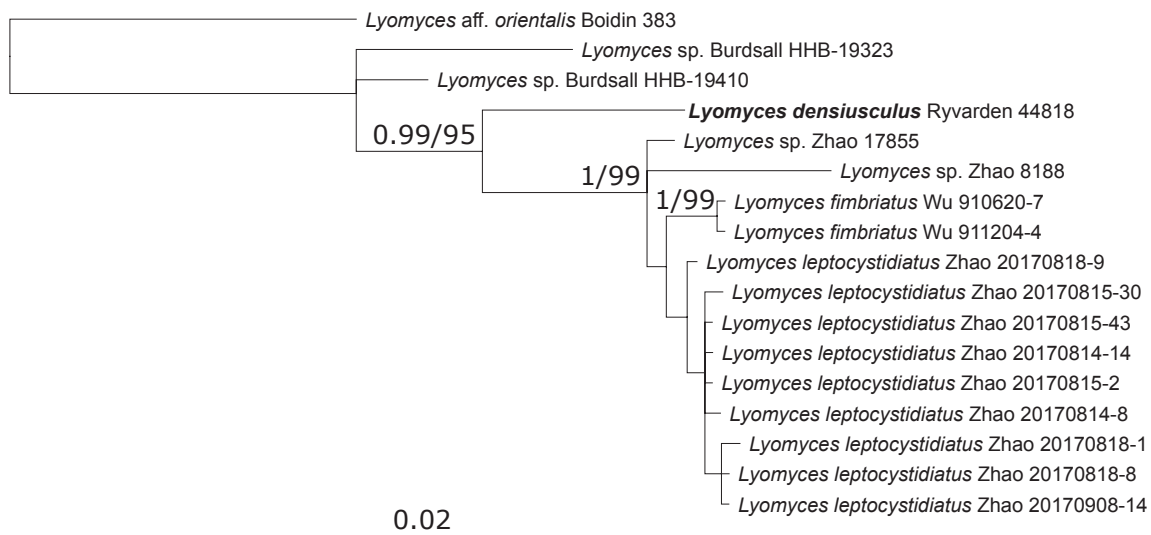


**Fig. 3.** Phylogenetic relationships of *Lyomyces densiusculus* and allied taxa inferred from ITS sequences using BI analysis. Bayesian posterior probabilities followed by ML bootstrap values are shown at nodes; branch lengths reflect estimated number of changes per site.

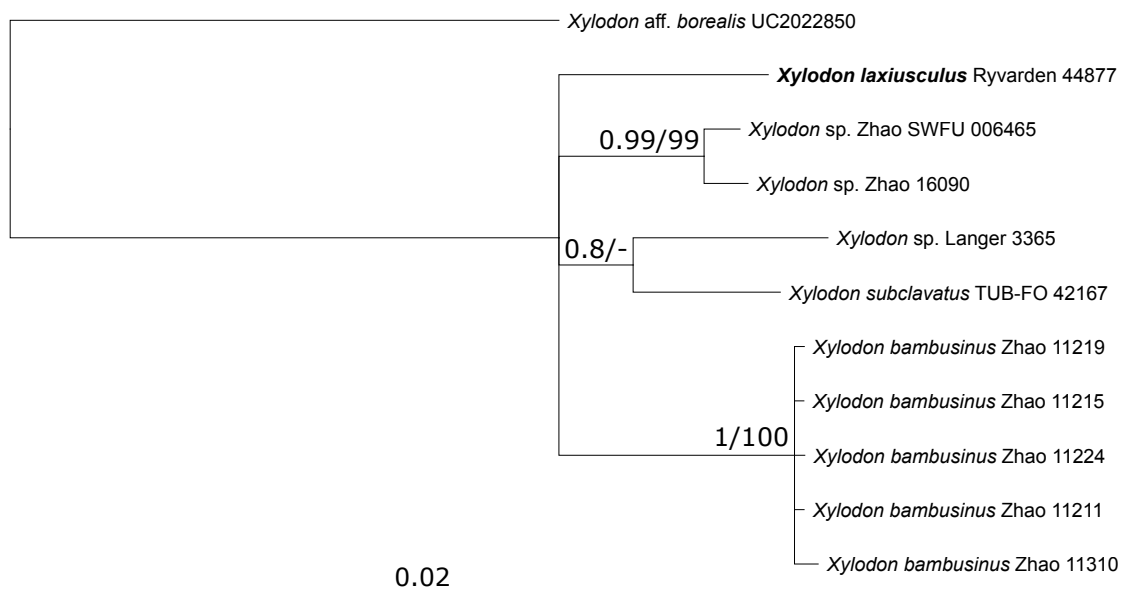


**Fig. 4.** Phylogenetic relationships of *Xylodon laxiusculus* and allied taxa inferred from ITS sequences using BI analysis. Bayesian posterior probabilities followed by ML bootstrap values are shown at nodes; branch lengths reflect estimated number of changes per site.

## TAXONOMY

***Lyomyces densiusculus*** Viner & Ryvarden, *sp. nov.* MycoBank MB 841943. Fig. 5.

**Etymology:** *Densiusculus* (Lat., adj.), a bit dense, refers to the dense and obscure hyphal system.

**Basidiocarp** effused, up to 6 cm in the widest dimension. Margin indistinct, hymenial surface cream to almost white, smooth to tuberculate; hymenophoral projections barely visible with an unaided eye, up to 70  $\mu\text{m}$  high, 50–80  $\mu\text{m}$  broad at base, 1–3 per mm. **Hyphal system** monomitic; hyphae clamped, thin- to thick-walled especially in subiculum (up to 1  $\mu\text{m}$ ). While being mostly obscure and densely packed, hyphal fragments of 4–5 cells may be observed at some places in subiculum and

subhymenium. Large clusters of crystalline matter sprinkled throughout the fruit-body obscure the hyphal structure even further. **Subhymenial hyphae** mostly obscure but those which can be seen, slightly cyanophilic, 1.8–3.3(–3.8)  $\mu\text{m}$  wide ( $n = 20/1$ ). **Subicular hyphae** not cyanophilic, branched mostly at right angles, 1.8–4.7  $\mu\text{m}$  wide ( $n = 19/1$ ). **Cystidial elements** from capitate to tapering, 13–21(–25)  $\times$  4–7  $\mu\text{m}$  ( $n = 23/1$ ), evenly distributed in and between hymenophoral projections. **Basidia** suburniform, 4-spored, 13–20  $\times$  4.2–6  $\mu\text{m}$  ( $n = 16/1$ ). **Basidiospores** thin-walled, narrowly ellipsoid to subcylindrical, slightly cyanophilic, 5.3–6.9(–7.2)  $\times$  3.1–4(–4.2)  $\mu\text{m}$  ( $n = 30/1$ ),  $L = 6.165$ ,  $W = 3.62$ ,  $Q = 1.7$ .

**Distribution and ecology:** Western Uganda, on bark of angiosperm branch. So far known only from the type locality.

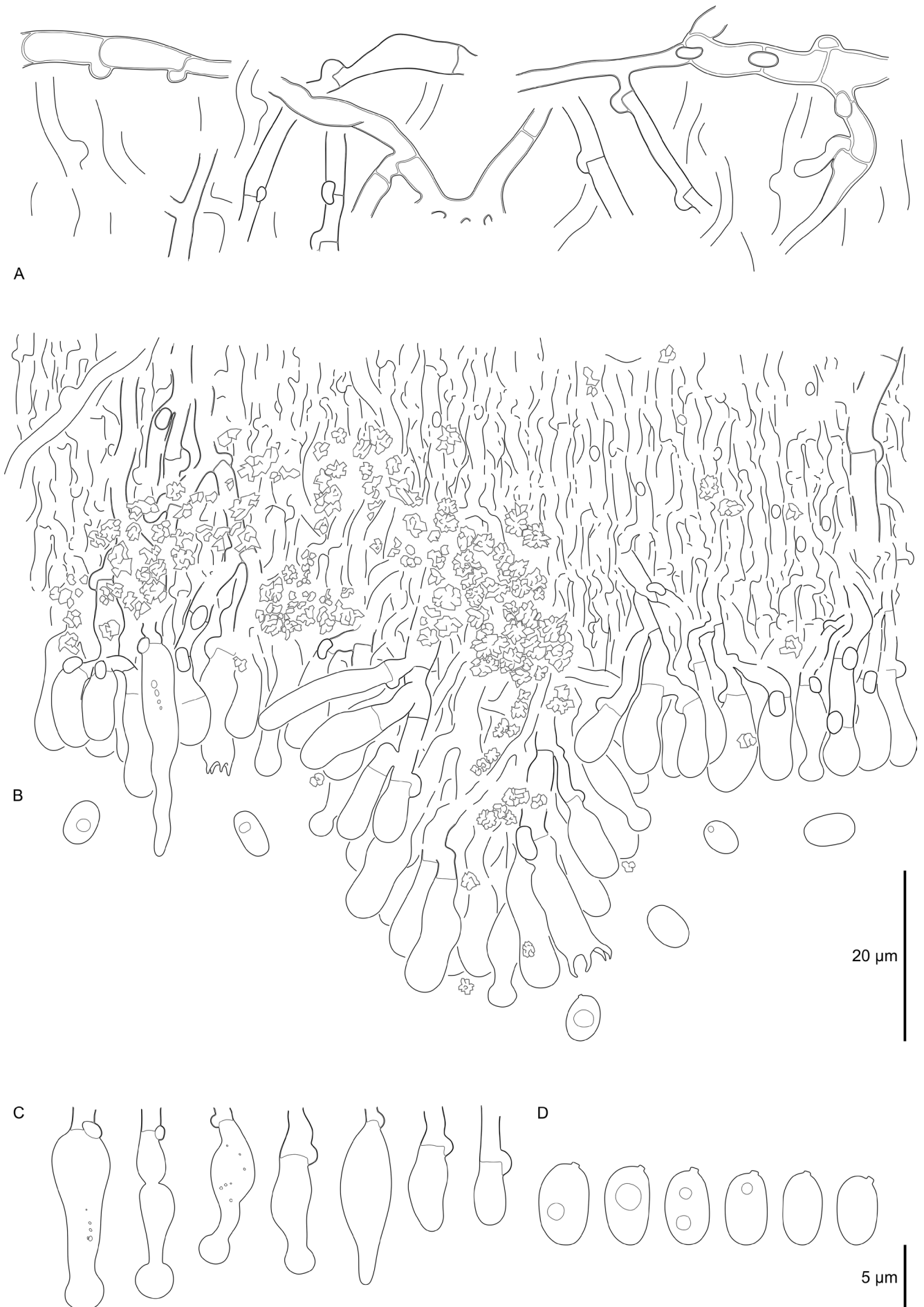


**Fig. 5.** *Lyomyces densiusculus* (holotype). **A.** Subiculum. **B.** Section of the sporocarp through hymenophoral projection and subhymenium. **C.** Sterile hymenophoral elements including cystidia of different shapes. **D.** Spores.

**Typus:** Uganda, Western Uganda, Kabarole district, Kibale National Park, Makerere University Field Station, on bark of angiosperm branch, 20 Apr. 2002, *L. Ryvardeen*, 44818 (**holotype** O, **isotype** in H) – ITS and 28S sequence, GenBank OK273853.

**Notes:** *Lyomyces densiusculus* resembles the *L. sambuci* species complex. Despite being recently addressed by Yurchenko *et al.* (2017) and Wang *et al.* (2021), some taxonomic problems in the *L. sambuci* complex still linger. According to the published data and our own observations, it contains several true species – undescribed or with existing old names – separated by DNA, morphology (at least in some cases), and ecological preferences. While making the decision to introduce *L. densiusculus* as a new species, we were guided by the following considerations. Morphologically, the combination of densely packed hyphae and subcylindrical spores allows separating this species from European or African collections of *L. sambuci* *s.l.* we are aware of. According to our molecular analyses, *L. densiusculus* is distant enough (the closest match is 94.6%, or 40 bp difference in ITS) from any sequences in public databases, as well as our unpublished sequences, to not belong to some recently described *Lyomyces*. We also studied the type of its closest relative *L. fimbriatus*, Wu 880729-13, described from Taiwan. It has grandinoid basidiocarps with fimbriate projections, more loose hyphal structure, well-differentiated long cystidia, and ellipsoid to broadly ellipsoid spores, altogether making distinguishing these two species easy.

***Xylodon angustisporus*** Viner & Ryvardeen, *sp. nov.* MycoBank MB 841321. Fig. 6.

**Etymology:** *Angustisporus* (Lat., adj.), narrow-spored, refers to the narrow spores.

**Basidiocarp** effused, up to 5 cm in the widest dimension. Margin indistinct, hymenial surface cream to almost light ochraceous, grandinoid; hymenophoral projections up to 200  $\mu$ m high, 150–200  $\mu$ m broad at base, 8–11 per mm. **Hyphal system** monomitic; hyphae clamped, distinct, thin- to thick-walled especially in subiculum (up to 1  $\mu$ m). **Subhymenial hyphae** cyanophilic, 1.5–3.5  $\mu$ m wide ( $n = 29/2$ ). **Subicular hyphae** slightly cyanophilic, branched mostly at right angles, (1.2–)2.1–4.6(–5)  $\mu$ m wide ( $n = 22/2$ ). A few subicular hyphae have large intercalary inflations, 7–10  $\mu$ m wide. Characteristic rounded crystals scattered through basidiocarp, 3–6  $\mu$ m in diam. Hymenial elements cyanophilic to strongly cyanophilic. **Cystidia** are of different shapes: from capitate and spatulate to obtuse and moniliform, 12–21.4(–35)  $\times$  (3.2–)3.5–5.5(–6.2)  $\mu$ m ( $n = 73/2$ ). Moniliform cystidia are mostly confined to the base of hymenophoral projections. Cystidia of all shapes sometimes have strongly cyanophilic contents and (or) thickened-walls (up to 0.8  $\mu$ m). Thick- to thin walled hyphidia make up the core of hymenophoral projections. Some thin walled hyphidia moderately to strongly flexuous. **Basidia** suburniform, 4-spored, 13–22  $\times$  3.9–5  $\mu$ m ( $n = 21/2$ ). **Basidiospores** thin-walled, narrowly ellipsoid to subcylindrical, slightly cyanophilic, (4.3–)4.8–6.2  $\times$  2.4–3.2  $\mu$ m ( $n = 63/2$ ),  $L = 5.2$ ,  $W = 2.4$ ,  $Q = 1.84$ .

**Distribution and ecology:** So far known only from Cameroon, on bark of angiosperms.

**Typus:** Cameroon, the East Region, Upper Nyong Division, Dja Biosphere Reserve, NW Dja sector, 3 km south of Somalomo, on

bark of angiosperm branch, 12 Sep. 2019, *L. Ryvardeen*, 50691B (**holotype** O, **isotype** in H) – ITS and 28S sequence, GenBank OK273831.

**Additional materials examined:** Cameroon, the Southwest Region, Ndiang Division, Korup National Park, on trail to transect P, lowland rain forest, on liana hanging down from high canopy, 2 Mar. 1991, *L. Ryvardeen*, 22729 (O).

**Notes:** *Xylodon angustisporus* is a sister taxon of *X. pruniaceus* (see below) described from eastern Africa, which differs only in the spore morphology and slightly more robust basidiocarps. *Xylodon angustisporus* might be confused with *X. nespori*, a species (or probably a species complex) with a wide intercontinental distribution. *Xylodon nespori* specimen Ryvardeen 22729 reported from Cameroon (Hjortstam *et al.* 1993), turned out to be *X. angustisporus*, thus further underlining the morphological similarity between the two species. Generally, *X. nespori* differs in spore morphology but, in our experience, some individuals of *X. nespori* from the Holarctic give spore measurements overlapping with *X. angustisporus*. Therefore, spores alone might not be characteristic enough. We find moniliform cystidia, flexuous hyphidia, slightly more dense hyphal structure, and hymenium with abundant strongly cyanophilic elements in *X. angustisporus* to be good distinguishing features between the two species.

***Xylodon dissiliens*** Viner & Ryvardeen, *sp. nov.* MycoBank MB 841330. Fig. 7.

**Etymology:** *Dissiliens* (Lat., adj.), bursting, refers to the cystidia, which easily collapse.

**Basidiocarp** effused, up to 5 cm in the widest dimension. Margin pruinose, grayish, while the rest of hymenial surface white, grandinoid; hymenophoral projections rather irregularly arranged, barely visible for the unaided eye, up to 100  $\mu$ m high, 80–100  $\mu$ m broad at base, 9–11(–13) per mm. **Hyphal structure** monomitic, hyphae clamped. **Subhymenial hyphae** thin-walled, slightly cyanophilic, (2.9–)3.4–5  $\mu$ m wide ( $n = 20/1$ ). **Subicular hyphae** slightly thick-walled, branched mostly at right angles 2.8–5  $\mu$ m wide ( $n = 20/1$ ). Large stellate crystals scattered throughout the basidiocarp. **Cystidia** of two types: a) large, thin-walled leptocystidia of subhymenial origin, from cylindrical to almost globose, sometimes with protuberances close to the apex, 20–43(–50)  $\times$  5–20(–25)  $\mu$ m ( $n = 21/1$ ); b) capitate cystidia in hymenium, often bearing a stellate crystalline cap, 14–26  $\times$  4–10  $\mu$ m ( $n = 20/1$ ). **Basidia** suburniform, 4-spored, 14–17.5  $\times$  4–5.5  $\mu$ m ( $n = 11/1$ ). **Basidiospores** thin-walled, ellipsoid, slightly cyanophilic, 5–6.3(–6.7)  $\times$  3.7–4.8  $\mu$ m ( $n = 30/1$ ),  $L = 5.5$ ,  $W = 4.16$ ,  $Q = 1.32$ . The whole basidiocarp structure is very delicate: most elements easily collapse if pressed too hard while mounting the slide. This is especially relevant for large leptocystidia, which burst first even when basidia and capitate cystidia are still intact.

**Distribution and ecology:** Western Uganda, on bark of angiosperm branch. So far known only from the type locality.

**Typus:** Uganda, Western Uganda, Kabarole district, Kibale National Park, Makerere University Field Station, on bark of angiosperm branch, 20 Apr. 2002, *L. Ryvardeen*, 44817 (**holotype** O, **isotype** in H) – ITS and 28S sequence, GenBank OK273856.



Fig. 6. *Xylodon angustisporus* (holotype). A. Section of the sporocarp through hymenophoral projection. B. Capitulate cystidia. C. Moniliform cystidia.

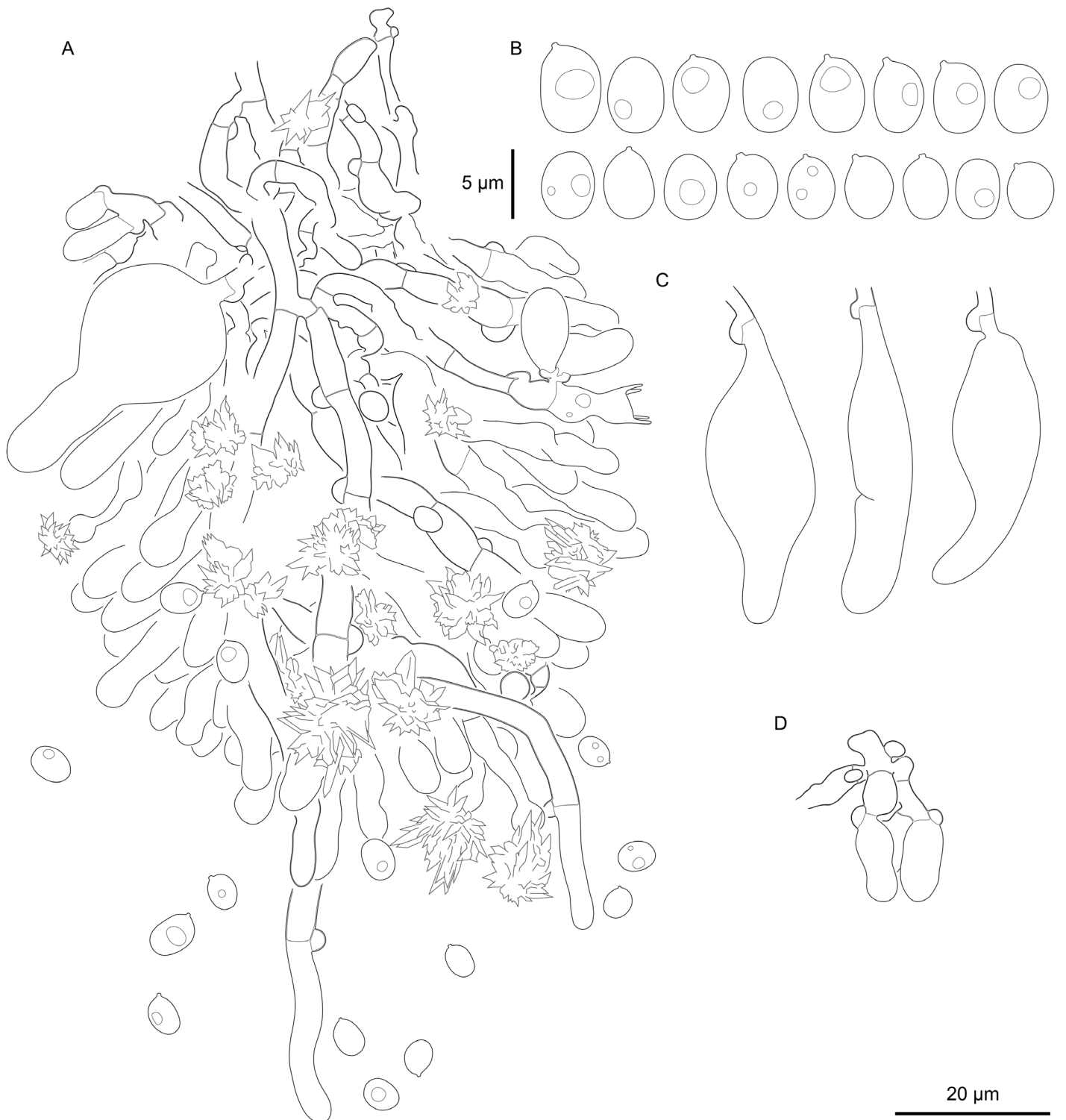


**Fig. 7.** *Xylodon dissiliens* (holotype). **A.** Section of the sporocarp through hymenophoral projection. **B.** Spores. **C.** Leptocystidia. **D.** Sterile hymenophoral elements.

**Notes:** Despite that the holotype Ryvarden 44817 was previously identified as *L. sambuci* s.l. (Ryvarden & Spirin 2019), the combination of readily collapsing lepto- and capitate cystidia with stellate crystalline cap makes *X. dissiliens* an easily distinguishable element in *Xylodon*. The presence of similar capitate cystidia resembles *X. detriticus*, *X. pruinosis*, and *X. ussuriensis*, another morphologically outlined group in the genus (the former *Lagarobasidium* Jülich).

***Xylodon laxiusculus*** Viner & Ryvarden, *sp. nov.* MycoBank MB 841331. Fig. 8.

**Etymology:** *Laxiusculus* (Lat., adj.), a bit loose, refers to the loose hyphal structure.

**Basidiocarp** effused, up to 4.5 cm in the widest dimension. Margin pruinose, white, while the rest of hymenial surface cream-coloured, grandinioid; hymenophoral projections rather irregularly arranged, hardly visible with an unaided eye, up to 50

$\mu\text{m}$  high, 50–70  $\mu\text{m}$  broad at base, 8–11 per mm. *Hyphal structure* monomitic, rather loose, hyphae clamped. *Subhymenial hyphae* thin-walled, slightly cyanophilic, 2.8–4.5  $\mu\text{m}$  wide ( $n = 21/1$ ). *Subicular hyphae* slightly thick-walled, branched mostly at right angles, (2.2–)2.8–4.5  $\mu\text{m}$  wide ( $n = 20/1$ ), rarely short-celled. Hyphae mostly naked, but loose clusters of rod-shaped crystals present on some subicular hyphae and more rarely in hymenium. Rare hyphal ends bear globose thin-walled swollen apex up to 6  $\mu\text{m}$  in diam. *Cystidia* irregular in shape, sometimes with several constrictions and (or) swollen apex 9–23.5(–28)  $\times$  (3–)3.7–6.2  $\mu\text{m}$  ( $n = 31/1$ ); some cystidia have protuberances close to the apex. A few cystidia have one clamped septum.

*Basidia* suburniform, 4-spored, 17–21  $\times$  4.1–5  $\mu\text{m}$  ( $n = 13/1$ ). *Basidiospores* thin-walled, ellipsoid, slightly cyanophilic, (4.2–)4.8–5.4  $\times$  (3–)3.8–4.3  $\mu\text{m}$  ( $n = 31/1$ ),  $L = 5.01$ ,  $W = 3.95$ ,  $Q = 1.27$ .

*Distribution and ecology*: Western Uganda, on angiosperm wood (fallen decorticated logs). So far known only from the type locality.

*Typus*: **Uganda**, Western Uganda, Kabarole district, Kibale National Park, Makerere University Field Station, on dead angiosperm wood, 20 Apr. 2002, L. Ryvarden 44877, (**holotype** O, **isotype** in H) – ITS sequence, GenBank OK273827.

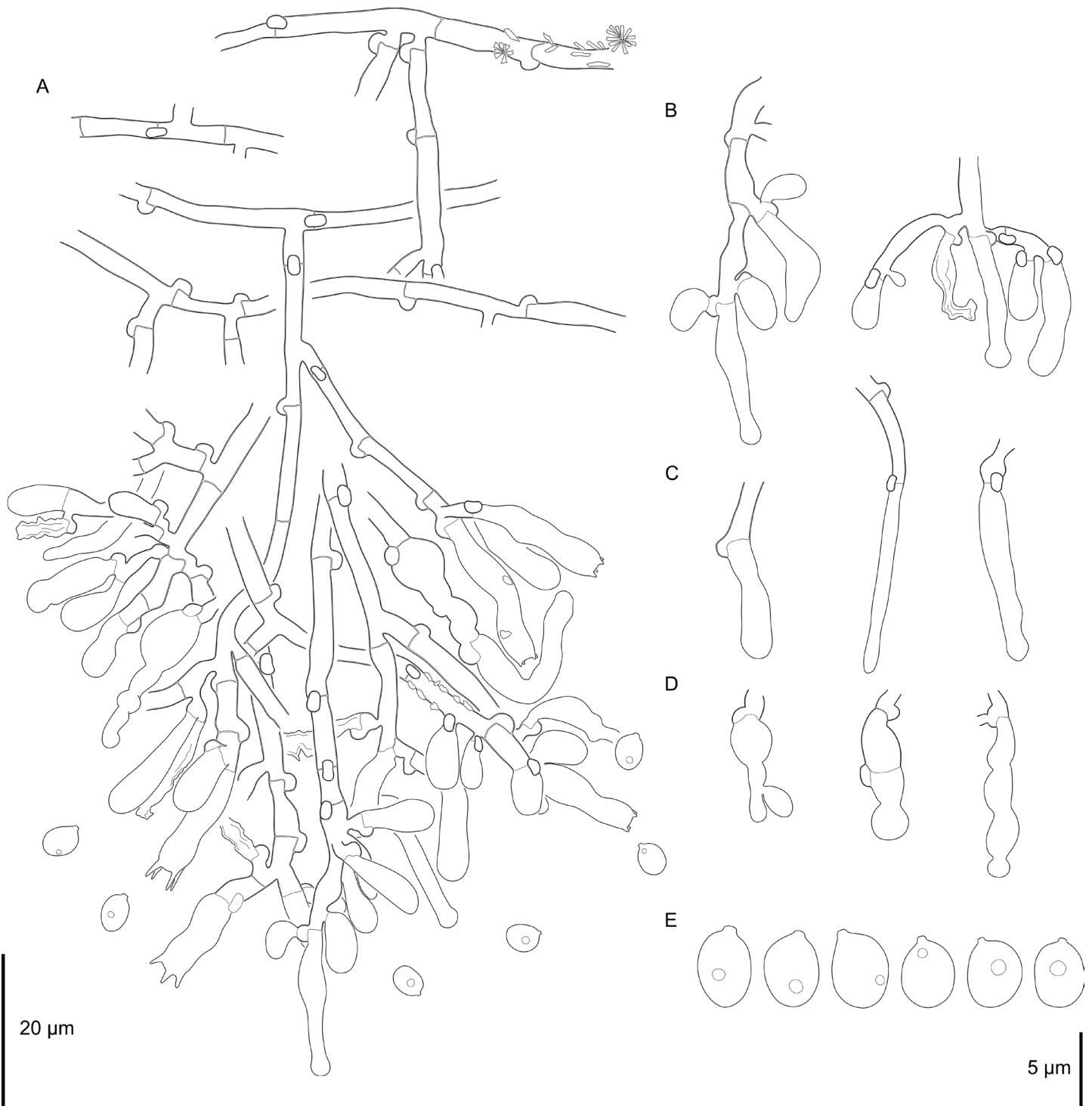


**Fig. 8.** *Xylodon laxiusculus* (holotype). **A.** Section of the sporocarp through hymenophoral projection. **B.** Clusters of sterile hymenophoral elements. **C.** Sterile hymenophoral elements. **D.** Cystidia. **E.** Spores.

*Notes:* We compared *X. laxiusculus* with collections of its closest match (93.8 % similarity or 41 bp difference in ITS), the Taiwanese species *X. subclavatus* (Wu 880310-1, 880510-2, 880516). *Xylodon laxiusculus* lacks most distinguishing features of the former. Those are odontoid hymenium, well-pronounced moniliform cystidia, and capitate hyphal ends with resinous cap. Macroscopically, *X. laxiusculus* is distinguished by loose (at margin almost porulose) fruit-body with hymenial projections visible only under the lens. *Xylodon laxiusculus* slightly resembles the conifer-dwelling *X. brevisetus*, but lacks its characteristic crystals and gloeocystidia. That was the reason why *X. laxiusculus* was initially reported as *X. brevisetus* s.l. (Ryvarden & Spirin 2019).

***Xylodon pruniaceus*** (Hjortstam & Ryvarden) Hjortstam & Ryvarden, *Syn. Fung.* (Oslo) **26**: 39. 2009.

*Basionym:* *Hyphodontia pruniacea* Hjortstam & Ryvarden, *Syn. Fung.* (Oslo) **18**: 25. 2004.

*Basidiocarp* effused, up to 5 cm in the widest dimension. Margin indistinct, hymenial surface cream to almost light ochraceous, grandinoid to odontoid; aculei up to 400 µm high, 150–250 µm broad at base, 5–7 per mm. *Hyphal system* monomitic; hyphae clamped, distinct, thin- to thick-walled especially in subiculum (up to 1.5 µm). *Subhymenial hyphae* cyanophilic, 1.7–4(–4.8) µm wide (n = 71/6). *Subicular hyphae*, slightly cyanophilic, branched mostly at right angles, 2–4.9 µm wide (n = 69/6). A few subicular hyphae have large intercalary inflations, 6–9 µm wide. Characteristic rounded crystals are scattered throughout the basidiocarp, 3–6 µm in diam. Hymenial elements cyanophilic to strongly cyanophilic. *Cystidia* are of different shapes: from capitate and spathulate to obtuse and moniliform, 11–25(–30) × 3–6 µm (n = 184/6). Moniliform cystidia are mostly confined to the base of hymenophoral projections. Cystidia of all shapes sometimes have strongly cyanophilic contents and (or) thickened-walls (up to 0.8 µm). Thick- to thin-walled hyphidia make up the core of hymenophoral projections. Some thin-walled hyphidia moderately to strongly flexuous. *Basidia* suburniform, 4-spored, 12–21 × 3.9–6 µm (n = 68/6). *Basidiospores* thin-walled, narrowly ellipsoid to subcylindrical, slightly cyanophilic, (3.5–)4.6–5.8(–6.9) × 2.8–3.8(–4.1) µm (n = 176/6), L = 5.14, W = 3.29, Q = 1.57.

*Distribution and ecology:* Previously reported only from the type locality in Tanzania, but several additional specimens from Tanzania and Malawi have been identified by us. The species grows on angiosperm wood.

*Typus:* **Tanzania**, Kilimanjaro Province, Mt. Kilimanjaro west slope, W. Kilimanjaro Forest Sta., alt. ca. 1 800 m, on angiosperm wood, 10–11 Feb. 1973, L. Ryvarden, 10223 (**holotype** K, **isotype** in O, studied).

*Additional materials examined:* **Malawi**, Southern Province, Zomba district, Zomba plateau, alt. ca. 1 500–1 700 m, on dead angiosperm wood, 7 Mar. 1973, L. Ryvarden, 11251 (H, O). **Tanzania**, Kilimanjaro Province, Mt. Kilimanjaro south slope above Mweka, alt. ca. 1 800–2 300 m, on angiosperm wood, 12 Feb. 1973, L. Ryvarden, 10286 (**paratype** in K, O); L. Ryvarden, 10301b (H, O); Mt. Kilimanjaro west slope, W. Kilimanjaro Forest Sta., alt. ca. 1 800 m, on angiosperm wood, 10 Feb. 1973, L. Ryvarden, 10216 (H, O); 11 Feb. 1973, L. Ryvarden, 10283 (H, O).

*Notes:* The species is very similar in almost all respects to its Western African relative *X. angustisporus* described above

and resembles the widely distributed *X. nespori*. The spore morphology of *X. pruniaceus* allows separating it from those two species.

***Xylodon submucronatus*** (Hjortstam & Renvall) Hjortstam & Ryvarden, *Syn. Fung.* (Oslo) **26**: 40. 2009.

*Basionym:* *Hyphodontia submucronata* Hjortstam & Renvall, *Edinb. J. Bot.* **55**: 481. 1998.

*Typus:* **Tanzania**, Arusha (Northern) Province, Arusha District, western side of Mt. Meru above Laikinoi, ridge between the streams Engare Olmotonyi and Engare Narok, in *Hagenia abyssinica* forest, alt. 2 800 m, fallen branch of *H. abyssinica*, 14 Dec. 1988, Renvall, 1602 (**holotype** H, **isotypi** in K, KUO, GB) – ITS sequence, GenBank OK273830.

*Additional materials examined:* **Kenya**, Central Province, Trans-Nzoia county, Mt. Elgon, south of the Suam River valley to Kapcalwa Gate, on dead angiosperm wood, 24 Jan. 1973, Ryvarden, 9322b (H, O).

*Notes:* The second collection of *X. submucronatus* reported in this study fits well with the description and illustration given by Niemelä *et al.* (1998). Its identity was further reaffirmed by our ITS analyses. This finding extends the known distribution of this species north up to Eastern Kenya. Despite its morphological similarity to *X. spathulatus* indicated by Niemelä *et al.* (1998), the closest match to *X. submucronatus* is *X. rimosissimus* (96 % similarity or 25 bp difference in ITS; Fig. 2). Thus, *X. submucronatus* appears to be a well-defined morphological species among known taxa allied to *X. rimosissimus*. On the other hand, sequences of *X. spathulatus* did not even pass the similarity threshold of 93 %.

## DISCUSSION

All published results suggest that the relationships within *Xylodon* and allied genera (including *Lyomyces*) are not well resolved when the ribosomal DNA loci are the sole source for genetic information. There has been a recent attempt to establish a reliable phylogeny of this group based on a comprehensive taxon sampling and multiple DNA loci by Wang *et al.* (2021). Their analysis of a concatenated dataset consisting of ITS, 28S, and mitochondrial small subunit (mtSSU) resolved *Lyomyces* and *Xylodon* as monophyletic genera. However, the analysis could suffer from a “gappy” alignment approach. Their large collection of partial gene sequences was assembled in a multiple sequence alignment containing a lot of missing data: a number of species were represented by just one or two loci while missing the remaining ones. Such a pattern of missing data could pose a major problem for the phylogenetic analysis (Hartmann & Vision 2008). Considering that Wang *et al.* (2021) have not mentioned any statistical methods compensating for the missing data, the existence of *Xylodon* and *Lyomyces* as two separate genera requires further investigation.

The addition of our four new species brings the number of currently recognized *Xylodon* and *Lyomyces* described from sub-Saharan Africa (including Réunion) to 10. Obviously, that number is not even close to the true diversity of this group on the continent. Considering that tropical Africa remains poorly explored for wood-inhabiting fungi, it is likely that many more *Xylodon* species will be found.

## ACKNOWLEDGEMENTS

We thank the anonymous reviewers of the manuscript for their useful comments. This research was supported by a University of Helsinki three-year research project (OM, IV) and Societas pro Fauna et Flora Fennica (IV). Karl-Henrik Larsson and Ellen Larsson (GB) kindly helped us with organizing a loan. Anton Savchenko (Tartu), Evgeniy Dunayev (Young Naturalist Club of the Zoological Museum, Lomonosov Moscow State University), Karl-Henrik Larsson, and Viacheslav Spirin (Helsinki) provided us with valuable fungal collections. Gaurav Sablok (Helsinki) helped us with the processing of genomic data.

**Conflict of interest:** The authors declare that there is no conflict of interest.

## REFERENCES

- Bankevich A, Nurk S, Antipov D, *et al.* (2012). SPAdes: a new genome assembly algorithm and its applications to single-cell sequencing. *Journal of computational biology* **19**: 455–477.
- Benson DA, Cavanaugh M, Clark K, *et al.* (2018). GenBank. *Nucleic Acids Research* **46**: D41–D47.
- Cheek M, Gosline G, Onana JM (2018). *Vepris bali* (Rutaceae), a new critically endangered (possibly extinct) cloud forest tree species from Bali Ngemba. Cameroon. *Willdenowia* **48**: 285–292.
- Cheek M, Nic Lughadha E, Kirk P, *et al.* (2020). New scientific discoveries: Plants and fungi. *Plants, People, Planet* **2**: 371–388.
- Chen S, Zhou Y, Chen Y, *et al.* (2018). fastp: an ultra-fast all-in-one FASTQ preprocessor. *Bioinformatics* **34**: 884–890.
- Katoh K, Rozewicki J, Yamada KD (2017). MAFFT online service: multiple sequence alignment, interactive sequence choice and visualization. *Briefings in Bioinformatics* **20**: 1160–1166.
- Landvik S (1996). *Neolecta*, a fruit-body producing genus of the basal ascomycetes, as shown by SSU and LSU rDNA sequences. *Mycological Research* **100**: 199–202.
- Li D, Liu CM, Luo R, *et al.* (2015). MEGAHIT: an ultra-fast single-node solution for large and complex metagenomics assembly via succinct de Bruijn graph. *Bioinformatics* **31**: 1674–1676.
- Lücking R, Hawksworth DL (2018). Formal description of sequence-based voucherless Fungi: promises and pitfalls, and how to resolve them. *IMA Fungus* **9**: 143–166.
- Harris RS (2007). *Improved pairwise alignment of genomic DNA*. Ph.D. dissertation. College of Engineering, the Pennsylvania State University, USA.
- Hartmann S, Vision TJ (2008). Using ESTs for phylogenomics: can one accurately infer a phylogenetic tree from a gappy alignment? *BMC Evolutionary Biology* **8**: 1–13.
- Hjortstam K, Ryvar den L (2007). Studies in corticioid fungi from Venezuela III (*Basidiomycotina*, *Aphyllorphorales*). *Synopsis Fungorum* **23**: 56–107.
- Hjortstam K, Ryvar den L (2009). A checklist of names in *Hyphodontia sensu stricto - sensu lato* and *Schizopora* with new combinations in *Lagarobasidium*, *Lyomyces*, *Kneiffiella*, *Schizopora*, and *Xylodon*. *Synopsis Fungorum* **26**: 33–55.
- Hjortstam K, Ryvar den L, Watling R (1993). Preliminary checklist of non-agaricoid macromycetes in the Korup National Park, Cameroon and surrounding area. *Edinburgh Journal of Botany* **50**: 105–119.
- Hopple JS, Vilgalys R (1994). Phylogenetic relationships among coprinoid taxa and allies based on data from restriction site mapping of nuclear rDNA. *Mycologia* **86**: 96–107.
- Kutuzova IA, Kokaeva LY, Pobendinskaya MA, *et al.* (2017). Resistance of *Helminthosporium solani* strains to selected fungicides applied for tuber treatment. *Journal of Plant Pathology* **99**: 635–642.
- Martin KJ, Rygielwicz PT (2005). Fungal-specific PCR primers developed for analysis of the ITS region of environmental DNA extracts. *BMC Microbiology* **5**: 1–11.
- Miettinen O, Niemela T, Spirin W (2006). Northern *Antrodiella* species: the identity of *A. semisupina*, and type studies of related taxa. *Mycotaxon* **96**: 211–240.
- Milne I, Lindner D, Bayer M, *et al.* (2008). TOPALi v2: a rich graphical interface for evolutionary analyses of multiple alignments on HPC clusters and multi-core desktops. *Bioinformatics* **25**: 126–127.
- Nguyen L-T, Schmidt HA, Von Haeseler A, *et al.* (2015). IQ-TREE: a fast and effective stochastic algorithm for estimating maximum-likelihood phylogenies. *Molecular Biology and Evolution* **32**: 268–274.
- Niemelä T, Renvall P, Hjortstam K (1998). *Hagenia abyssinica* and its fungal decayers in natural stands. *Edinburgh Journal of Botany* **55**: 473–484.
- Riebesehl J, Langer E (2017). *Hyphodontia s.l. (Hymenochaetales, Basidiomycota)*: 35 new combinations and new keys to all 120 current species. *Mycological Progress* **16**: 637–666.
- Ronquist F, Teslenko M, Van Der Mark P, *et al.* (2012). MrBayes 3.2: efficient Bayesian phylogenetic inference and model choice across a large model space. *Systematic Biology* **61**: 539–542.
- Ryvar den L, Spirin V (2019). Studies in *Aphyllorphorales* of Africa 39. Some corticioid species from Uganda. *Synopsis Fungorum* **39**: 38–40.
- Stein F (1969). Particle size measurements with phase contrast microscopy. *Powder Technology* **2**: 327–334.
- Wang XW, May TW, Liu SL, *et al.* (2021). Towards a natural classification of *Hyphodontia sensu lato* and the trait evolution of basidiocarps within *Hymenochaetales* (*Basidiomycota*). *Journal of Fungi* **7**: 478.
- White TJ, Bruns T, Lee S, *et al.* (1990). Amplification and direct sequencing of fungal ribosomal RNA genes for phylogenetics. In: *PCR protocols: A guide to the methods and applications* (Innis MA, Gelfand DH, Sninsky JJ, White TJ, eds). Academic Press. New York: 315–322.
- Yurchenko E, Riebesehl J, Langer E (2017). Clarification of *Lyomyces sambuci* complex with the descriptions of four new species. *Mycological Progress* **16**: 865–876.